

Available online at [www.sciencedirect.com](http://www.sciencedirect.com)

ScienceDirect

[www.elsevier.com/locate/jes](http://www.elsevier.com/locate/jes)

**JES**  
 JOURNAL OF  
 ENVIRONMENTAL  
 SCIENCES  
[www.jesc.ac.cn](http://www.jesc.ac.cn)

## Effects of typical algae species (*Aphanizomenon flosaquae* and *Microcystis aeruginosa*) on photoreduction of $\text{Hg}^{2+}$ in water body

Rongguo Sun<sup>1,2</sup>, Yafei Mo<sup>2</sup>, Xinbin Feng<sup>1,\*</sup>, Leiming Zhang<sup>3</sup>, Lin Jin<sup>2</sup>, Qiuhua Li<sup>2</sup>

1. State Key Laboratory of Environmental Geochemistry, Institute of Geochemistry, Chinese Academy of Sciences, Guiyang, China

2. School of Chemistry and Material, Guizhou Normal University, Guiyang, China

3. Air Quality Research Division, Science and Technology Branch, Environment and Climate Change Canada, Toronto, Ontario, Canada

### ARTICLE INFO

#### Article history:

Received 22 August 2018

Revised 24 January 2019

Accepted 14 February 2019

Available online 26 February 2019

#### Keywords:

*Aphanizomenon flosaquae*

*Microcystis aeruginosa*

Photoreduction

Divalent inorganic mercury ( $\text{Hg}^{2+}$ )

### ABSTRACT

Photoreduction characteristics of divalent inorganic mercury ( $\text{Hg}^{2+}$ ) in the presence of specific algae species are still not well known. Laboratory experiments were conducted in the present study to identify the effects of different concentrations of living/dead algae species, including *Aphanizomenon flosaquae* (AF) and *Microcystis aeruginosa* (MA), on the photoreduction rate of  $\text{Hg}^{2+}$  under various light conditions. The experimental results showed that percentage reduction of  $\text{Hg}^{2+}$  was significantly influenced by radiation wavelengths, and dramatically decreased with the presence of algae. The highest percentage reduction of  $\text{Hg}^{2+}$  was induced by UV-A, followed by UV-B, visible light and dark for both living and dead AF, and the order was dark > UV-A > UV-B > visible light for both living and dead MA. There were two aspects, i.e., energy and attenuation rate of light radiation and excrementitious generated from algae metabolisms, were involved in the processes of  $\text{Hg}^{2+}$  photoreduction with the presence of algae under different light conditions. The percentage reduction of  $\text{Hg}^{2+}$  decreased from 15% to 11% when living and dead AF concentrations increased by 10 times (from  $10^6$  to  $10^5$  cells/mL), and decreased from 11% to ~9% in the case of living and dead MA increased. Algae can adsorb  $\text{Hg}^{2+}$  and decrease the concentration of free  $\text{Hg}^{2+}$ , thus inhibiting  $\text{Hg}^{2+}$  photoreduction, especially under the conditions with high concentrations of algae. No significant differences were found in percentage reduction of  $\text{Hg}^{2+}$  between living and dead treatments of algae species. The results are of great importance for understanding the role of algae in  $\text{Hg}^{2+}$  photoreduction.

© 2019 The Research Center for Eco-Environmental Sciences, Chinese Academy of Sciences.

Published by Elsevier B.V.

### Introduction

Mercury (Hg) is a highly toxic heavy metal, which can cause detrimental impacts on human and ecosystem health once it enters into aquatic bodies through industrial waste water

discharges and atmospheric deposition (Wright et al., 2018). Environmental Hg pollution and its biogeochemical cycling have attracted much attention since the occurrence of Minamata disease (Liu et al., 2012, 2018). Elemental mercury ( $\text{Hg}^0$ ) has an approximate atmospheric residence time of

\* Corresponding author. E-mail: [fengxinbin@vip.skleg.cn](mailto:fengxinbin@vip.skleg.cn). (Xinbin Feng).

0.5–1 year (O'Driscoll et al., 2005) and thus can be transported globally, causing Hg pollution even in remote areas (Beckers and Rinklebe, 2017). Hg<sup>0</sup> released across water–air surface is predominantly stimulated by photoreduction of divalent inorganic mercury (Hg<sup>2+</sup>) (Yin et al., 2011). Therefore, the photoreduction of Hg<sup>2+</sup> plays an important role in the biogeochemical cycle of Hg.

Hg<sup>2+</sup> reduced to Hg<sup>0</sup> under UV (280–400 nm) and visible light (400–700 nm) conditions are first- to second-order kinetic reactions (Carla et al., 2015; Zhang, 2006; Zhu et al., 2018). Many factors, such as light conditions, dissolved organic matter, coexisting ions, and biological processes, can influence the photoreduction of Hg<sup>2+</sup> in water environments (Vost et al., 2012). Algae is a key factor in the process of Hg<sup>2+</sup> photoreduction in aquatic systems, especially in eutrophic waters where algae are abundant (Lalonde et al., 2004). There are many biologically active and functionalized groups, such as cellulose, pectin substance, alginic acid ammonium salt, polysaccharide, and polygalactose sulphate, on cell surfaces of algae (Deng et al., 2008, 2009; Zeraatkar et al., 2016). Meanwhile, algae have large surface areas with negatively charged cell surface, enabling them to be excellent absorbent to Hg<sup>2+</sup>, which will reduce reactive mercury species in water column (Schartup et al., 2017; Soerensen et al., 2016). Therefore, if the above hypothesis is correct in reality, the reduction rate of Hg<sup>2+</sup> may decrease in the presence of algae. To date, the characteristics of photoreduction of Hg<sup>2+</sup> in the presence of certain algae species are still not well known.

Light radiation has been shown to be an important factor affecting the processes of Hg<sup>2+</sup> photoreduction (Qureshi et al., 2009; Vost et al., 2012). A wide range of wavelengths including UV-A (365 nm), UV-B (310 nm), and visible light interact with dissolved organic matter (DOM), coexisting ions (Fe<sup>3+</sup>, Cl<sup>-</sup>, NO<sub>3</sub><sup>-</sup>, etc.), and algae, thereby generating hydrogen peroxide, hydroxyl radicals, and singlet oxygen, etc., a process that can significantly affect photoreduction of Hg<sup>2+</sup> (Vost et al., 2012; Zhang, 2006). Light radiation is needed in the process of photosynthesis and thus is also important for the growth of algae. The reaction characteristics of Hg<sup>2+</sup> reduction under different wavelengths in the presence of algae are still unknown.

Another question is that whether there are any differences in the effects algae on photoreduction of Hg<sup>2+</sup> between living and dead algae species. Hg<sup>2+</sup> can cross cell membrane and enter into algae cells by passive transport. In addition, living algae can excrete small organic molecules, such as alginate, halochlamydosan, polypeptide, etc. The excretions also include some free electrons, i.e., hydrated electron (e<sub>aq</sub><sup>-</sup>), hydrogen peroxide (H<sub>2</sub>O<sub>2</sub>), singlet oxygen (<sup>1</sup>O<sub>2</sub>), and superoxide anion (O<sub>2</sub><sup>-</sup>) (Deng et al., 2008). These excretions can affect the photoreduction of Hg<sup>2+</sup> through coordinated interactions with small organic molecules and oxidation with free electrons (Vost et al., 2012). However, dead algae do not have such physiological activity, which may cause potential differences between living and dead algae in their impacts on photoreduction of Hg<sup>2+</sup>.

To address the knowledge gaps outlined above, laboratory experiments were designed to characterize Hg<sup>2+</sup> reduction under different wavelength ranges in the presence of living/dead algae species, *Aphanizomenon flosaquae* (AF) and

*Microcystis aeruginosa* (MA), both of which are typical algae species in eutrophic water systems. The effects of adsorption process of Hg<sup>2+</sup> by algae cells on the photoreduction of Hg<sup>2+</sup> were also determined.

## 1. Materials and methods

### 1.1. Experimental materials and devices

A 500-mL quartz glass gas cylinder (diameter 7.2 cm, height 15 cm) was used as the reactor (Fig. 1). The Teflon tubing (Savilleux, US) was used as the conduit. Trace mercury was removed by a gold trap amalgam before the carrier gas entering into the reactor. Hg<sup>0</sup> generated by the Hg<sup>2+</sup> reduction reaction was separated by high-purity argon (Ar), dried by soda lime (Sigma-Alorich, Germany), and then concentrated onto a gold-coated sand trap. The trapped Hg<sup>0</sup> was thermally desorbed from the gold sample trap into an inert gas stream (Ar) that carried the released Hg<sup>0</sup> in the cell of a cold-vapor atomic fluorescence spectrometry (CVAFS) for detection (Model III, Brooks Rand Labs, USA) (EPA, 2002; Sun et al., 2014). UV-A (365 nm, 30 W), UV-B (310 nm, 30 W) and Xenon (visible light, 30 W) lamps were used as light sources. The lamps were 45.5 cm away from the bottle wall. All the bottles were wrapped in tin foil and placed in a dark environment for dark treatment. The temperature of all solutions was 25°C and all experiments were conducted under ambient temperature of 25 ± 0.5°C.

The algal species tested in the present study were AF (Fig. 2A) and MA (Fig. 2B), which were cultured in BG-11 liquid culture medium at 25°C, with illumination intensity of 4000 Lux and the light/dark ratio of 12:12 hr. AF was supposed to be cylindrical with average length and diameter being measured as 9 and 2.23 μm, respectively. MA was supposed to be spherical with average diameter being measured as 3.42 μm. Cell surface area to volume ratio was evaluated to be 1.58 and 1.75 μm<sup>2</sup>/μm<sup>3</sup>, respectively, for AF and MA.

### 1.2. Experimental design and methods

The algal samples in stable growth stage were washed and filtrated repeatedly, and then divided into two groups. Algal samples in one group were killed but the cell walls remained intact by water bath caefaction at 50°C for 10 min. The algae concentrations of both groups were diluted to several levels, including 1.0 × 10<sup>6</sup>, 2.0 × 10<sup>6</sup>, 4.0 × 10<sup>6</sup>, 8.0 × 10<sup>6</sup>, and 10.0 × 10<sup>6</sup> cells/mL. The cell walls of two algae species kept integrity during a 1440 min period by microscopic observations.

200 mL living/dead algae solution and 20 μL mercury chloride (HgCl<sub>2</sub>, 1000 ng/mL, GR) solution were mixed into the reactor, which was then quickly connected to the pipes as shown in Fig. 1. Light source was turned on simultaneously when high purity argon was added into reaction solution (0.10 L/min). The analytical gold-coated sand trap was replaced at time phases of 20, 60, 120, 240, and 1440 min for measurements. The experimental design is presented in Table 1.

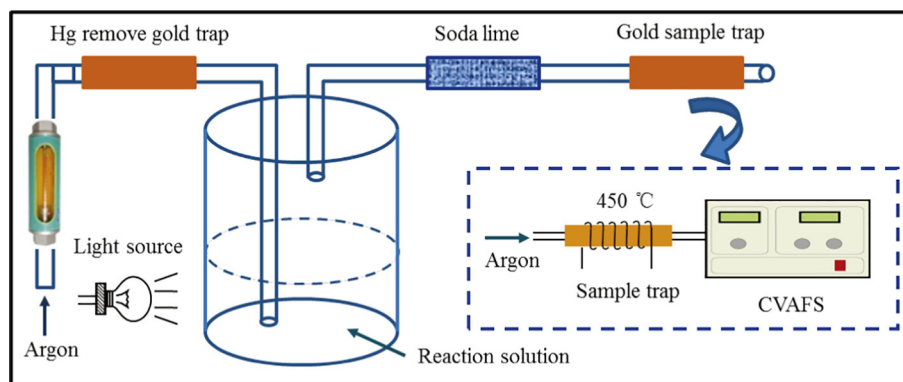


Fig. 1 – Schematic diagram of the reaction device.

Adsorption abilities of algae for  $\text{Hg}^{2+}$  were also characterized. 200 mL living/dead algae solution ( $4.0 \times 10^6$  cells/mL) and 20  $\mu\text{L}$  mercury chloride ( $\text{HgCl}_2$ , 1000 ng/mL, GR) solution were added into quartz triangular flask, which was then shaken at a constant speed (120 r/min) under dark condition at the temperature of 25°C. 10 mL solution was sampled from the reactor at every time phase of 20, 60, 120, 240, and 1440 min and then transferred into 10 mL centrifuge tubes (Yonggong, Jiangsu, China). Supernatants were extracted by centrifugation at 4000 r/min for 5 min. The concentrations of total  $\text{Hg}^{2+}$  in supernatants were determined following the procedures presented in the method 1631 (EPA, 2002). The blank control experiments were conducted using ultrapure water with no algae in the solution. Initial pH values were measured to be 6.3–6.7 for all the experiments.

### 1.3. Quality control and data analysis

All glass instruments were immersed in 25% nitric acid for 24 hr and then burned in a muffle furnace at 500°C for more than 4 hr before being used, and they were used for only once after naturally cool down in a Hg-free environment. Disposable gloves were worn to prevent cross-contamination. The processes of quality control followed the method 1631 (EPA, 2002). The percentage reduction of  $\text{Hg}^{2+}$  (%) was calculated as the ratio of total mass of  $\text{Hg}^0$  (ng)/initial amount of  $\text{Hg}^{2+}$  (ng).

The reaction order was calculated according to the first- and second-order reaction formula (Lu et al., 2004). All the data were analyzed with SPSS 22.0 software for Windows.

## 2. Results

### 2.1. Effects of wavelength

The total mass of  $\text{Hg}^0$  produced during the 1440 min period under various light conditions ranged from 2.05 to 2.92 ng in the presence of AF, and from 1.81 ng to 2.76 ng in the presence of MA. The order of the produced total  $\text{Hg}^0$  mass was UV-A > UV-B > visible light > dark for both living and dead AF, and was dark > UV-A > UV-B > visible light for both living and dead MA (Fig. 3A and B). For blank control, the highest  $\text{Hg}^0$  yield was induced by UV-B radiation (5.35 ng), followed by UV-A (4.57 ng), visible light (4.29 ng), and dark (4.08 ng) (Fig. 3C). Variance analysis showed significant differences in the total mass of the produced  $\text{Hg}^0$  between the different treatments of algae under various light conditions ( $p < 0.05$ ).

The  $\text{Hg}^0$  production rates within the first 20 min experiments in the presence of algae were calculated to be  $(6.35\text{--}8.46) \times 10^{-4}$  ng/min under dark,  $(6.73\text{--}9.13) \times 10^{-4}$  ng/min under UV-A,  $(5.16\text{--}8.71) \times 10^{-4}$  ng/min under UV-B, and  $(5.16\text{--}7.57) \times 10^{-4}$  ng/min under visible light. Higher  $\text{Hg}^0$  production

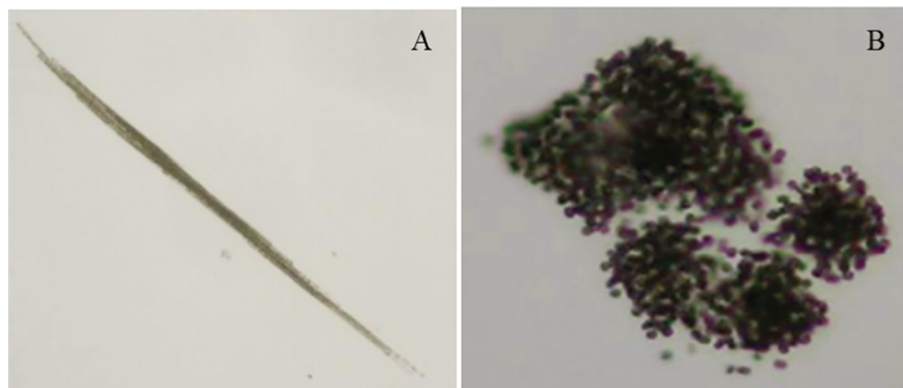


Fig. 2 – *Aphanizomenon flosaquae* (A) and *Microcystis aeruginosa* (B).

**Table 1 – Experiments conducted.**

Objectives	Concentrations of algae species (cells/mL)	Wavelength
Identify the effects of wavelength	$1.0 \times 10^6$	UV-A, UV-B, visible light, and dark
Identify the effects of algae concentrations	$1.0 \times 10^6$ , $2.0 \times 10^6$ , $4.0 \times 10^6$ , $8.0 \times 10^6$ , and $10.0 \times 10^6$	UV-A
Blank control	0	UV-A, UV-B, visible light, and dark

rates by 1.2–2.8 folds were found for blank control experiments than with algae treatments under various light conditions in this time frame. The  $\text{Hg}^0$  production rate within 240–1440 min under various light conditions were calculated to be  $(3.40\text{--}3.81) \times 10^{-3}$  ng/min for blank control and  $(1.51\text{--}2.43) \times 10^{-3}$  ng/min for algae treatments. These results suggested that  $\text{Hg}^0$  production rates were significantly influenced by radiation wavelength, and dramatically decreased with the presence of algae.  $\text{Hg}^0$  production rates were higher in the initial stage than later times during the experiment period.

The percentage reduction of  $\text{Hg}^{2+}$  under different light conditions was in the decreasing order of UV-A (14.60%) > UV-B (14.06%) > visible light (13.68%) > dark (10.26%) with living AF, dark (13.78%) > UV-A (10.97%) > UV-B (10.73%) > visible light (9.07%) with living MA, UV-A (14.61%) > UV-B (14.26%) > visible light (13.30%) > dark (10.68%) with dead AF, and dark (13.72%) > UV-A (11.40%) > UV-B (10.92%) > visible light (9.30%) with dead MA (Fig. 4). Thus, the percentage reduction of  $\text{Hg}^{2+}$  varied under different wavelengths regardless of with (or without) living or dead algae. For blank control experiment, the highest percentage reduction of  $\text{Hg}^{2+}$  was induced by UV-B (26.75%), followed by UV-A (22.86%), visible light (21.45%), and dark (20.41%) (Fig. 4). Comparing results of blank control experiment with those with algae treatments, it

was found that the presence of algae inhibited  $\text{Hg}^{2+}$  photoreduction. Variance analysis elucidated significant differences in the percentage reduction of  $\text{Hg}^{2+}$  between various light conditions ( $P < 0.05$ ), indicating wavelength was an important factor impacting the photoreduction of  $\text{Hg}^{2+}$  with or without algae.

## 2.2. Effects of algae concentrations

When the AF concentrations were given as 0,  $1.0 \times 10^6$ ,  $2.0 \times 10^6$ ,  $4.0 \times 10^6$ ,  $8.0 \times 10^6$ , and  $10.0 \times 10^6$  cells/mL, the respective total mass of  $\text{Hg}^0$  produced were calculated to be 4.57, 2.92, 2.65, 2.59, 2.33, and 2.20 ng for living AF treatments, and were 4.57, 2.92, 2.69, 2.53, 2.37, and 2.25 ng for dead AF treatments (Fig. 5 A). The same tendencies as listed above were also found for the cases with living or dead MA, i.e., total mass of  $\text{Hg}^0$  produced decreased with increasing algae concentrations. Note that there were no significant differences in the total mass of produced  $\text{Hg}^0$  between the cases of living and dead algae treatments ( $p > 0.05$ ). The total mass of  $\text{Hg}^0$  produced with treatments of living AF, dead AF, living MA, and dead MA decreased by 52%, 51%, 62%, and 61%, respectively, compared with that from the blank control during the 1440 min period (Fig. 5). Correlation analysis showed that total mass of  $\text{Hg}^0$

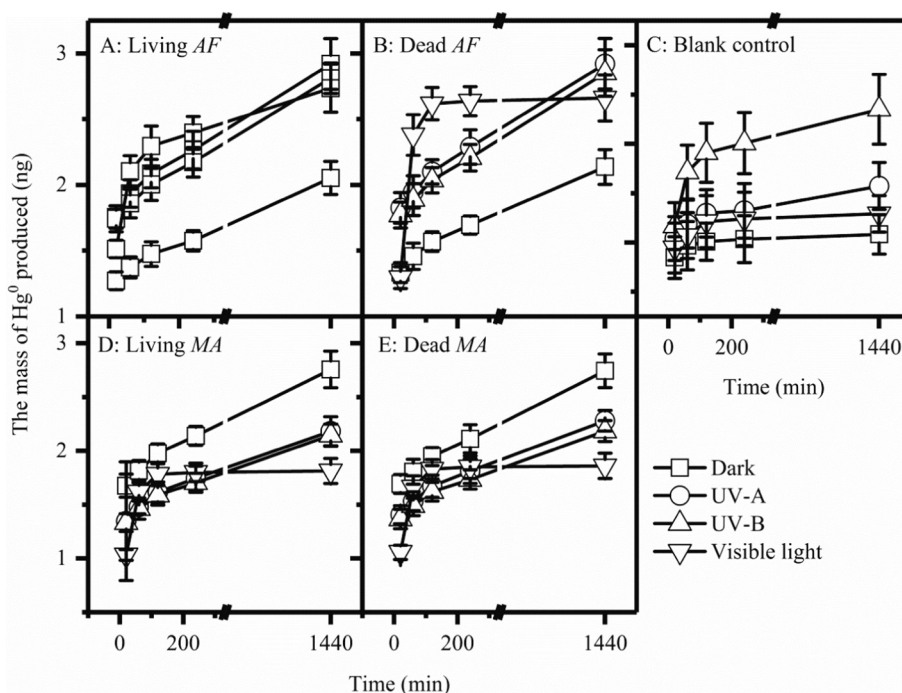


**Fig. 3 – Characteristics of the total mass of  $\text{Hg}^0$  produced under different illumination conditions during 0–1440 min period in the presence of algae.**



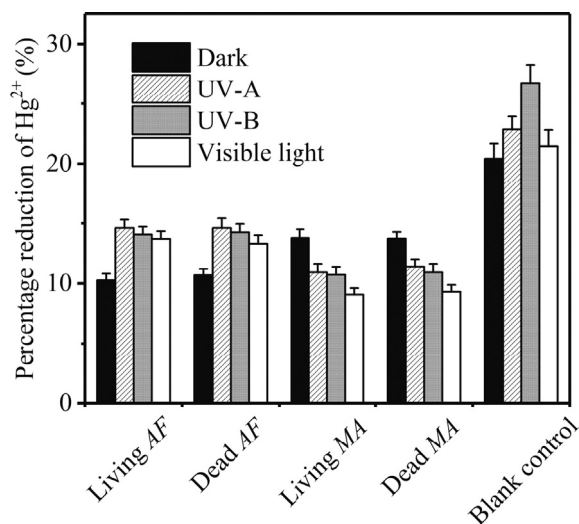


**Fig. 4 – Percentage reduction of Hg<sup>2+</sup> under different wavelengths of light radiation during the period of 0–1440 min.**

produced were negatively correlated to algae concentrations, suggesting that algae species played a key role in controlling the photoreduction of Hg<sup>2+</sup>, especially at high concentrations. Hg<sup>0</sup> production rates within 240 min period were calculated to be in the range of (5.75–9.53) × 10<sup>-3</sup> ng/min from all the algae treatments experiments, which were much lower than that from the

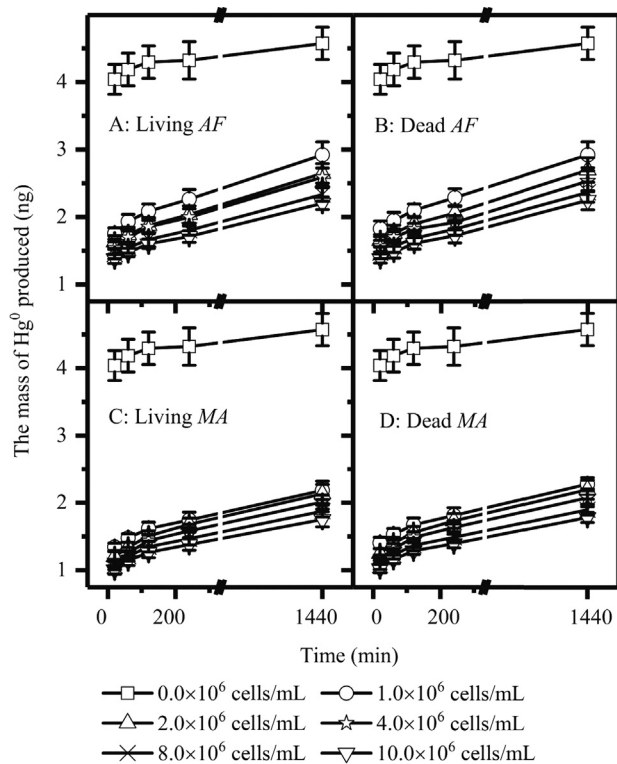


**Fig. 5 – Characteristics of Hg<sup>0</sup> production with the presence of various algae concentrations under UV-A radiation during the period of 0–1440 min.**

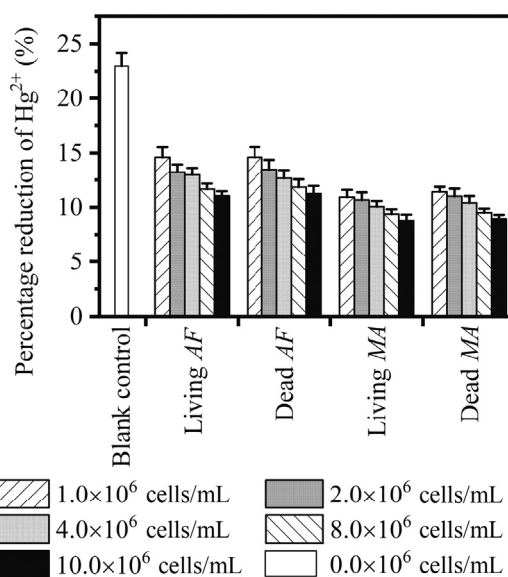


**Fig. 6 – Percentage reduction of Hg<sup>2+</sup> with the presence of various algae concentrations under UV-A radiation during the period of 0–1440 min.**

blank control experiment (18.01 × 10<sup>-3</sup> ng/min). The production rates decreased significantly during the rest of the experiment periods ((0.21–0.55) × 10<sup>-3</sup> ng/min) for all the treatments.

A significant decreasing tendency was seen in the percentage reduction of Hg<sup>2+</sup> with increasing algae concentrations (Fig. 6). The percentage reduction of Hg<sup>2+</sup> decreased from 15% to 11% when living and dead AF concentrations increased by one order of magnitude from 1.0 × 10<sup>6</sup> to 1.0 × 10<sup>7</sup> cells/mL, and decreased from 11% to 9% in the case of living and dead MA increased. These results indicated that small differences in Hg<sup>2+</sup> photoreduction reaction were caused by different algae species. The peak value (22.86%) of percentage reduction of Hg<sup>2+</sup> was found in the case without algae in reaction solution (Fig. 6).

### 3. Discussion

#### 3.1. Effects of wavelength

Solar radiation intensity and its wavelength are of great importance for mercury photoreduction in water system (Vost et al., 2012). Photochemical reactions can be either primary or secondary in nature (Zhang, 2006). Ultraviolet radiation is important in aquatic chemistry because of its ability to efficiently induce primary and secondary photochemical reactions in aquatic ecosystems (Häder et al., 2007). Under natural UV light, Hg<sup>2+</sup>, such as Hg(OH)<sub>2</sub>, HgSO<sub>3</sub>, and Hg(HSO<sub>3</sub>)<sup>-</sup>, can all undergo reduction reactions to generate dissolved gaseous mercury (DGM) in natural water systems (Sun et al., 2015). Ultraviolet light promotes the production of DGM (Sun et al., 2015), of which 61%–73% were produced under UV light, and a maximum of 27% was produced under visible light (Garcia et al., 2005). Initial work suggested that UV-A radiation was primarily responsible for mercury reductive reactions because DGM production rates did not change significantly by

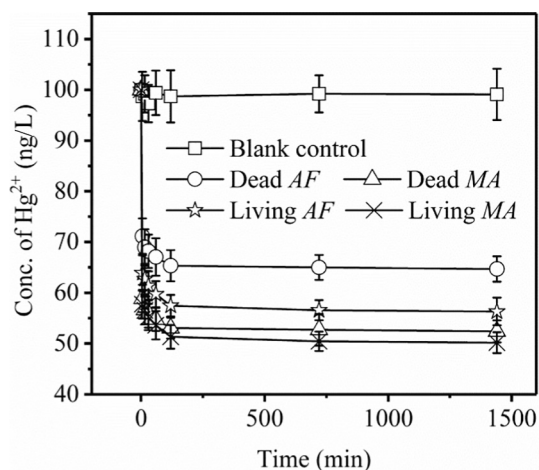


**Fig. 7 – Concentrations of Hg<sup>2+</sup> in supernatants for adsorption experiment during the period of 0–1440 min.**

the removal of UV-B radiation using a Mylar screen (Amyot et al., 1994). A recent study suggested that UV-B radiation was a key portion of electromagnetic spectrum responsible for mercury reduction in freshwaters (Vost et al., 2012). The controlled radiation experiments in freshwaters found that Hg<sup>2+</sup> photoreduction rate constant was higher for UV-B radiation than for UV-A radiation (O’driscoll et al., 2006a; O’Driscoll et al., 2006b). At present, the exact mechanism of UV light-induced Hg<sup>2+</sup> photoreduction is still unclear.

Indeed, Hg<sup>2+</sup> photoreduction rate is affected by a combination of the wavelength and intensity of radiation, the chemical composition of water body, the concentration and structure of chromophores in the natural water, and the rate of attenuation of specific radiation wavebands (Vost et al., 2012). UV-B radiation is shorter in wavelength and higher in energy than UV-A radiation (Vost et al., 2012). The 6s orbital of mercury is assumed to be the acceptor orbital in all wavelength ranges, resulting in different excited states generated via transitions from the steady state by absorbing different spectrum (Sun et al., 2014; Zhang, 2006). Therefore, we found that the highest percentage reduction of Hg<sup>2+</sup> was induced by UV-B radiation, followed by UV-A radiation, visible light and dark in the absence of algae species. However, the presence of algae species disturbed this order. Incident radiation of UV-B radiation was lower than that of UV-A radiation because of the more-rapid attenuation of UV-B. The reaction rates with the presence of AF were thus higher under UV-A radiation than UV-B radiation. The energies of quantum photon of visible light were too low to induce photoreduction of Hg<sup>2+</sup>, in contrast to the case found under UV radiations. Under dark conditions, there were no quantum photons to excite photochemical reactions. Therefore, the percentage reduction of Hg<sup>2+</sup> with the presence of AF were in the decreasing order of UV-A > UV-B > visible light > dark. As for the cases with the presence of MA, some other processes affected photoreduction of Hg<sup>2+</sup>. Highly reactive radicals, i.e., hydrated electrons (e<sub>aq</sub><sup>-</sup>), superoxide anion (O<sub>2</sub><sup>-</sup>), hydrogen peroxide (H<sub>2</sub>O<sub>2</sub>), and singlet oxygen (<sup>1</sup>O<sub>2</sub>), which were generated from some algae metabolisms Eqs. (1)–(4), can inhibit the process of Hg<sup>2+</sup>

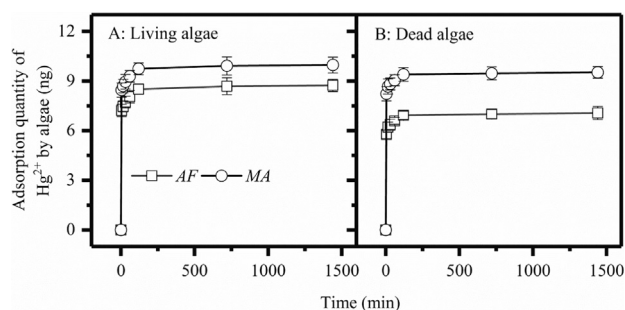


**Fig. 8 – Adsorption quantity of Hg<sup>2+</sup> by AF and MA during the period of 0–1440 min.**

reduced to Hg<sup>0</sup> under light conditions. Thus, the highest percentage reduction of Hg<sup>2+</sup> was found under dark condition with the presence of MA. Some other factors, such as metabolisms of algae and mercury–algae complex reactions, or some other mechanisms may also be involved in Hg<sup>2+</sup> photoreduction, resulting in very complex processes with the presence of algae species, especially in natural water systems. Investigating the roles of specific algae in the photoreduction processes of Hg<sup>2+</sup> is of great importance for understanding biogeochemical and cycling characteristics of mercury.



### 3.2. Effects of adsorption

The concentrations of Hg<sup>2+</sup> in supernatants decreased significantly in all the treatments with the presence of living and dead algae, but did not change in the blank control experiment during the 1440 min experiment period (Fig. 7). This demonstrates that adsorption process played a key role in decreasing the concentrations of free Hg<sup>2+</sup> in water. The adsorption quantity of Hg<sup>2+</sup> by the algae cells rapidly increased during the first 5 min. The adsorption quantity was 1.45 ng higher from living than dead AF (7.22 vs. 5.77 ng), and 0.22 ng higher for the case of MA (8.45 vs. 8.23 ng) (Fig. 8). The changes in the adsorption amounts slowed down during 5–120 min and tended to stabilize during 120–1440 min. The respective concentrations of Hg<sup>2+</sup> decreased to 56.31 and 50.16 ng/L at 1440 min in the presence of living AF and MA, and to 64.67 and 52.38 ng/L in the presence of dead AF and MA. This showed that the highest adsorbing capacity of adsorbent was living MA, followed by dead MA, living AF, and dead AF. Such differences in the adsorbing capacity between the two algae species were due to the higher cell surface area to volume ratio of MA than AF, and thus greater capacity for adsorbing Hg<sup>2+</sup>.

The adsorption of Hg<sup>2+</sup> by algae cells mainly consists of passive extracellular adsorption and active accumulation. Passive adsorption is the predominant process with a

relatively fast rate (Diéguez et al., 2013).  $\text{Hg}^{2+}$  adsorbed on cell surface of dead algae is the same as the process of passive adsorption by living algae (Zeraatkar et al., 2016). The living algae can adsorb  $\text{Hg}^{2+}$  through active accumulation as well as passive extracellular adsorption. Both adsorption processes can decrease the concentrations of free  $\text{Hg}^{2+}$ , thus declining the percentages of reduced  $\text{Hg}^{2+}$ . Although the adsorption processes are somewhat different between living and dead algae, no significant differences were found in the percentage reduction of  $\text{Hg}^{2+}$  in our experiments, indicating that after the addition of  $\text{HgCl}_2$ , the adsorption of  $\text{Hg}^{2+}$  by living and dead algae cells were mainly passive adsorption. This is because the process of active accumulation is very slow and plays a negligible role in the reactions. Algae may affect the concentration and structure of available DOM, thereby changing the chemical conditions of the photoreaction (Vost et al., 2012). If biological process is the major factor in affecting  $\text{Hg}^{2+}$  photoreduction, the reaction rates should change slowly in the initial stage and then change quickly at later stages because metabolism of algae could further change the chemical conditions. Photobiological reduction by algae may be mainly controlled by the excretion of small organic molecules and free electrons (Vost et al., 2012). Previous studies have identified no difference in DGM production between the presence of either diatom and its isolated exudates (Deng et al., 2008; Lanzillotta et al., 2004). Thus, physical adsorption is believed to be the predominant process after adding  $\text{HgCl}_2$ .

The cell wall of algae contains polysaccharides, proteins, amino, carbonyl, carboxyl, sulfhydryl, etc. groups that can bind to  $\text{Hg}^{2+}$  and adsorb  $\text{Hg}^{2+}$  to the cell wall (Schartup et al., 2017). Deng et al. (2008) found that the photoreduction rate of  $\text{Hg}^{2+}$  increased with the increasing concentration of *Anabaena*, and an opposite trend was found in the present study, likely due to the different cell structures of different algae species used here, which have different adsorption effect on  $\text{Hg}^{2+}$  photoreduction. AF and MA belong to Cyanophyta, which has a good adsorption effect on heavy metals (Zeraatkar et al., 2016), and thus has a certain influence on the photochemical reaction of  $\text{Hg}^{2+}$ . pH value may be an important factor affecting adsorption because of its influence on surface charge and cation exchange capacity. However, pH value was around 6.5 and did not change much during the whole 1440 min experiment period, preventing us from conducting further in-depth analysis on this issue. Whether DGM can be adsorbed on algae surface or not remain unclear in our experiment. Future research should focus on identifying species and concentrations of Hg in algae cell and estimating the role of algae species in biogeochemistry of Hg in water environment system.

#### 4. Conclusions

Light radiation had an important influence on the reduction of  $\text{Hg}^{2+}$ , and the effects of different light wavelengths on the reduction process of  $\text{Hg}^{2+}$  were quite different. The photoreduction of  $\text{Hg}^{2+}$  was inhibited by *Aphanizomenon flosaquae* (AF) and *Microcystis aeruginosa* (MA) with more obvious inhibitory

effects identified under high algae concentrations. The percentage reduction of  $\text{Hg}^{2+}$  was higher in the presence of AF than MA, suggesting algae species being an important factor in  $\text{Hg}^{2+}$  photoreduction. There were no significant differences between living and dead algae treatments as indicated by their similar reaction rates. Algae can adsorb  $\text{Hg}^{2+}$  and thus decrease the concentrations of free  $\text{Hg}^{2+}$  in solution, however, it is not clear whether the produced  $\text{Hg}^0$  was generated from the photoreduction of free  $\text{Hg}^{2+}$  in solution or from algae–Hg complexes. The biogeochemistry of algae–Hg complexes should be explored further.

#### Acknowledgements

This study was supported by the Science and Technology Department of Guizhou Province (No. Qiankehe LH zi [2017]7334 hao), the China Postdoctoral Science Foundation (No. 2017M613005), Foundation of Guizhou Educational Committee (No. Qian jiao he KY[2016]135), the National Natural Science Foundation of China (No. 41563012), and the Doctoral Scientific Research Foundation of Guizhou Normal University for 2014.

#### REFERENCES

- Amyot, M., McQueen, D.J., Mierle, G., Lean, D.R., 1994. Sunlight-induced formation of dissolved gaseous mercury in lake waters. *Environ. Sci. Technol.* 28 (13), 2366–2371.
- Beckers, F., Rinklebe, J., 2017. Cycling of mercury in the environment: sources, fate, and human health implications: a review. *Crit. Rev. Env. Sci. Tec.* 47 (10), 693–734.
- Carla, H.R., Sanghamitra, G., Joel, D.B., Bridget, A.B., 2015. Effects of ultraviolet radiation on mercury isotope fractionation during photo-reduction for inorganic and organic mercury species. *Chem. Geol.* 405, 102–111.
- Deng, L., Wu, F., Deng, N.S., Zuo, Y.G., 2008. Photoreduction of mercury(II) in the presence of algae, *Anabaena cylindrical*. *J. Photochem. Photobiol. B.* 91 (2–3), 117–124.
- Deng, L., Fu, D., Deng, N., 2009. Photo-induced transformations of mercury (II) species in the presence of algae, *Chlorella vulgaris*. *J. Hazard. Mater.* 164 (2), 798–805.
- Diéguez, M.C., Queimalios, C.P., Guevara, S.R., Marvin-DiPasquale, M., Cárdenas, C.S., Arribére, M.A., 2013. Influence of dissolved organic matter character on mercury in incorporation by planktonic organisms: an experimental study using oligotrophic water from Patagonian lakes. *J. Environ. Sci.* 25 (10), 1980–1991.
- García, E., Amyot, M., Ariya, P.A., 2005. Relationship between DOC photochemistry and mercury redox transformations in temperate lakes and wetlands. *Geochim. Cosmochim. Acta* 69 (8), 1917–1924.
- Häder, D., Kumar, H., Smith, R., Worrest, R., 2007. Effects of solar UV radiation on aquatic ecosystems and interactions with climate change. *Photochem. Photobiol. Sci.* 6 (3), 267–285.
- Lalonde, J.D., Amyot, M., Orvoine, J., Morel, F.M.M., 2004. Photoinduced oxidation of  $\text{Hg}^0$  (aq) in the waters from the St. Lawrence Estuary. *Environ. Sci. Technol.* 38 (2), 508–514.
- Lanzillotta, E., Ceccarini, C., Ferrara, R., Dini, F., Frontini, F., Banchetti, R., 2004. Importance of the biogenic organic matter in photo-formation of dissolved gaseous mercury in a culture of the marine diatom *Chaetoceros* sp. *Sci. Total Environ.* 318 (1–3), 211–221.

- Liu, G., Cai, Y., O'Driscoll, N., 2012. Overview of mercury in the environment. *Environ. Chem. Toxicol. Mercury* 1–12.
- Liu, K., Wang, S., Wu, Q., Wang, L., Ma, Q., Zhang, L., et al., 2018. A highly resolved mercury emission inventory of Chinese coal-fired power plants. *Environ. Sci. Technol.* 52 (4), 2400–2408.
- Lu, X.Y., Liu, J.L., Feng, M., 2004. *Physical Chemistry*. Chemical Industry Press, Beijing, pp. 214–252 (in Chinese).
- O'Driscoll, N.J., Rencz, A.N., Lean, D.R., 2005. Mercury cycling in a wetland dominated ecosystem: a multidisciplinary study. *Soc. of Environ. Toxicol. and Chem. Press*, Pensacola, Florida. 1–16.
- O'Driscoll, N., Siciliano, S., Lean, D., Amyot, M., 2006a. Gross photoreduction kinetics of mercury in temperate freshwater lakes and rivers: application to a general model of DGM dynamics. *Environ. Sci. Technol.* 40 (3), 837–843.
- O'Driscoll, N., Siciliano, S., Peak, D., Carignan, R., Lean, D., 2006b. The influence of forestry activity on the structure of dissolved organic matter in lakes: implications for mercury photoreactions. *Sci. Total Environ.* 366 (2), 880–893.
- Qureshi, A., O'Driscoll, N.J., MacLeod, M., Neuhold, Y.M., Hungerbühler, K., 2009. Photoreactions of mercury in surface ocean water: gross reaction kinetics and possible pathways. *Environ. Sci. Technol.* 44 (2), 644–649.
- Schartup, A., Qureshi, A., Dassuncao, C., Thackray, C., Harding, G., 2017. A model for methylmercury uptake and trophic transfer by marine plankton. *Environ. Sci. Technol.* 52 (2), 654–662.
- Soerensen, A.L., Schartup, A.T., Gustafsson, E., Gustafsson, B.G., Undeman, E., Bjorn, E., 2016. Eutrophication increases phytoplankton methylmercury concentrations in a coastal sea—a Baltic Sea case study. *Environ. Sci. Technol.* 50 (21), 11787–11796.
- Sun, R., Wang, D., Mao, W., Zhao, S., Zhang, C., 2014. Roles of chloride ion in photo-reduction/oxidation of mercury. *Chin. Sci. Bull.* 59 (27), 3390–3397.
- Sun, R., Wang, D., Mao, W., Ma, M., Zhang, C., Jiang, T., 2015. Diurnal characteristics of migration and transformation of mercury and effects of nitrate in Jialing River, Chongqing, China. *Chemosphere* 119, 634–641.
- US EPA, 2002. Method 1631: Mercury in Water by Oxidation, Purge and Trap, and Cold Vapor Atomic Fluorescence Spectrometry. Washington, DC. pp. 1–42.
- Vost, E.E., Amyot, M., O'Driscoll, N.J., 2012. Photoreactions of mercury in aquatic systems. *Environ. Chem. Toxicol. Mercury* 193–218.
- Wright, L.P., Zhang, L., Cheng, I., Aherne, J., Wentworth, G.R., 2018. Impacts and effects indicators of atmospheric deposition of major pollutants to various ecosystems - a review. *Aerosol Air Qual. Res.* 18, 1953–1992.
- Yin, Y., Li, Y., Cai, Y., Jiang, G., 2011. Environmental photochemistry of mercury. *Environ. Chem.* 30 (1), 173–177 in Chinese.
- Zeraatkar, A.K., Ahmadzadeh, H., Talebi, A.F., Moheimani, R.N., McHenry, M.P., 2016. Potential use of algae for heavy metal bioremediation, a critical review. *J. Environ. Manag.* 181, 817–831.
- Zhang, H., 2006. Photochemical Redox Reactions of Mercury. *Recent Developments in Mercury Science*. Springer, pp. 37–79.
- Zhu, S., Zhang, Z., Žagar, D., 2018. Mercury transport and fate models in aquatic systems: a review and synthesis. *Sci. Total Environ.* 639, 538–549.